Theory of the influence of end conditions on self-contact in DNA loops

Bernard D. Coleman, Irwin Tobias, and David Swigon
Department of Mechanics and Materials Science and Department of Chemistry, Rutgers, The State University of New Jersey, Piscataway, New Jersey 08854

(Received 17 April 1995; accepted 22 August 1995)

Explicit solutions of the equations of Kirchhoff's theory of elastic rods are employed to derive properties of the tertiary structure of a looped segment of DNA that is subject to geometric constraints imposed at its end points by bound proteins. In appropriate circumstances small changes in such boundary data cause a nearly planar loop to undergo a continuous and reversible transition that can be described as a 180° rotation taking the loop from an uncrossed to a singly crossed structure in which sequentially separated base pairs are brought into proximity. Expressions are derived relating points and angles of crossing to end conditions, and results are presented that facilitate the calculation of changes in elastic energy during such transitions. © *1995 American Institute of Physics.*

I. INTRODUCTION

We are concerned here with the tertiary structure of duplex DNA for cases in which a protein or a protein aggregate is bound to two sites of a DNA molecule in such a way that the otherwise free DNA segment between the points of contact with the protein forms a loop. Continuing the investigation of a recent paper,[1] referred to as (I), we treat the looped DNA segment as an homogeneous inextensible elastic body obeying the rod theory of Kirchhoff,[2–5] and we examine the nature of the dependence of its equilibrium tertiary structure on geometric conditions imposed at its end points. These conditions are of a strong anchoring type in which both position and orientation in space are specified for the base pairs at the ends of the segment.

Much is yet to be learned about the structures and modes of action of proteins that are known to bind to and induce deformations in DNA. Among the protein aggregates that appear to impose end conditions of the type discussed here are (i) those about which wrap lengths of DNA containing over 100 base pairs, such as the type II topoisomerase, DNA gyrase,[6,7] and the histone octamer,[8–12] and (ii) those formed when protein molecules bound to two distant sites of a DNA molecule come together to form a dimer, as is the case for several multipartite regulatory systems[13] for control of gene expression that are accompanied by DNA looping (see, e.g., recent papers[14,15] on the *lac* repressor–operator complex).

In each configuration the points on the axis of the rod representing the segment of double stranded DNA form a curve $\mathscr{C}$ which is described by giving the radial vector $\mathbf{r}$ from an origin $\mathbf{O}$ to a point on $\mathscr{C}$ as a function of arc-length s. The point at which $s=0$ is taken to be the midpoint of $\mathscr{C}$, and thus $-L/2$ and $L/2$, with L the length of $\mathscr{C}$, are the values of s at the end points of $\mathscr{C}$, which identify the two places where the otherwise free DNA segment is in contact with the protein structure. The conditions imposed at the end points are such that not only the radial vectors, $\mathbf{r}(-L/2)$ and $\mathbf{r}(L/2)$, but also the unit vectors tangent to $\mathscr{C}$ at its end points, $\mathbf{t}(-L/2)$ and $\mathbf{t}(L/2)$, are specified.

Let $\mathscr{P}$ be the plane in space containing the end points and midpoint of $\mathscr{C}$. In the present paper emphasis is laid on cases in which the tangents at the end points, $\mathbf{t}(-L/2)$ and $\mathbf{t}(L/2)$, have the same angle of inclination from $\mathscr{P}$, and that angle, β, is small, but not necessarily zero. Small changes in the distance between the end points of $\mathscr{C}$, or in the spherical coordinates that determine $\mathbf{t}(-L/2)$ and $\mathbf{t}(L/2)$, can result in large changes in the equilibrium tertiary structure of the DNA segment with axial curve $\mathscr{C}$. Particularly in the case of a nicked segment of duplex DNA, i.e., a segment that does not support a twisting moment because one of its two strands has been severed, this change can take the form of a smooth and reversible transition from the uncrossed axial curve labeled S_I in Fig. 1 to the crossed axial curve there labeled S_V. In (I) it was observed that the theory of such transitions suggests mechanisms for the activity of the topoisomerase, DNA gyrase. In the present paper we treat in a quantitative way the fact that in the transition $S_I \rightarrow S_V$ sequentially distant groups of base pairs are brought together at the point of crossing seen in S_V. We show below that, in the limit of planar configurations, i.e., in the limit in which β is zero, one can calculate the dependence of the arc-length coordinates of the sites that are brought into contact at the point of crossing, and the angle χ of contact, on the geometric conditions imposed where the DNA molecule departs from its region of contact with protein. We examine this dependence in detail, for it is hoped that a quantitative understanding of it will aid in the construction of models for action at a distance in the regulation of gene expression during transcription.

After giving in Sec. II a brief summary of our approach to the attainment of explicit solutions in the theory of the elastic-rod model for equilibrium tertiary structures of DNA segments, we present, in Sec. III, an apparently new, and strikingly simple, expression for the dependence of the total elastic energy of a rod at equilibrium on integration constants that are related to the end conditions. In subsequent sections the expression is employed to study the energetics of transitions between crossed and uncrossed configurations. A method of obtaining the integration constants from end conditions is described in Secs. IV and V and there applied to calculate shapes and energies of twist-free but nonplanar configurations.

In Sec. VI we present a way of treating planar configurations as limits of three-dimensional configurations for

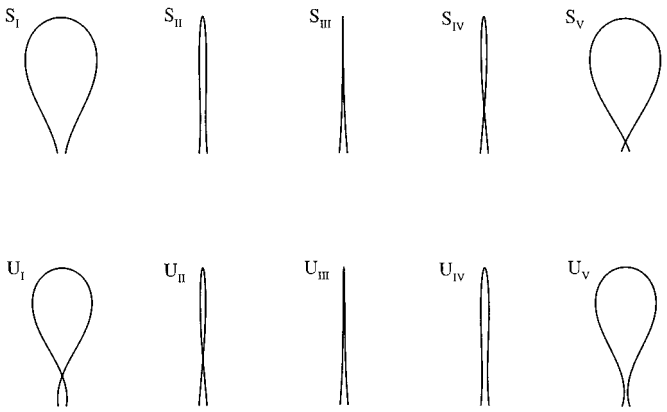

FIG. 1. Calculated axial curves $\mathscr{C}$ for stable (S_I,...,S_V) and unstable (U_I,...,U_V) equilibrium configurations of a nicked segment of DNA of fixed length L with $\eta=0.025$, $\beta=2°$ and values of α given in Table I. The view is along a line perpendicular to the plane $\mathscr{P}$ containing the end points $s=\pm L/2$ and the midpoint $s=0$ of $\mathscr{C}$.

which the tangent vectors at the end points and the vector connecting the end points approach vectors that lie in a common plane. We there derive the expressions relating points of crossing and angles of contact to parameters obtained from the end conditions. As one would expect, as the limit of coplanarity of boundary conditions is approached, transitions from crossed to uncrossed configurations become more abrupt. In the course of our examination of the energetics of the transitions for that limit, we derive an easily applied rule that determines, for nicked segments with the ratio η of the distance between the endpoints of $\mathscr{C}$ to the length L of $\mathscr{C}$ less than 0.1, whether a stable equilibrium configuration is crossed or uncrossed.

II. EQUILIBRIUM CONFIGURATIONS

In the present theory a segment of DNA is treated as a rod with cross sections that in a stress-free reference configuration are congruent and such that the two principal moments of inertia of each cross section are equal. It is assumed that the elastic response of the rod corresponds to that of a material with a symmetry group implying transverse isotropy about the rod axis. It is further assumed, for simplicity, that the rod is materially homogeneous and is ''naturally straight'' in the sense that in its stress-free reference configuration the axial curve $\mathscr{C}$ is an interval of a straight line. We use Kirchhoff's theory of inextensible rods,[2,3] which yields field equations complete to first-order in an appropriate dimensionless measure of thickness, curvature, and extension.[4,5]

Let $\mathbf{F}(s)$ be the resultant of the internal contact forces acting on the cross section of the rod characterized by arc-length coordinate s and $\mathbf{M}(s)$ the net moment of those forces. For a rod subject to no external forces or moments except at its end points, the general equations of mechanical equilibrium reduce to the assertions that $\mathbf{F}$ is independent of s and that

$$\mathbf{M}'=\mathbf{F}\times\mathbf{t}, \tag{1}$$

where $\mathbf{M}'=d\mathbf{M}/ds$, and $\mathbf{t}$ is the unit tangent vector, $\mathbf{t}=\mathbf{r}'$. Kirchhoff's constitutive equation for rods that are naturally straight here reduces to the following relation between $\mathbf{M}$ and the twist density Ω:

$$\mathbf{M}=A(\mathbf{t}\times\mathbf{t}')+C(\Omega-\Omega_o)\mathbf{t}. \tag{2}$$

The coefficient of flexural rigidity, A, and the coefficient of torsional rigidity, C, are constants; Ω_0 is the twist density characteristic of torsionally relaxed DNA. It follows from Eqs. (1) and (2) that $\mathbf{M}\cdot\mathbf{t}$ and Ω are independent of s. For duplex DNA that has been nicked, or, more generally, for a polymer molecule that cannot support a twisting moment, one may employ Eq. (2) with $\Omega=\Omega_o$, in which case $\mathbf{M}=A(\mathbf{t}\times\mathbf{t}')$.

It follows from Eq. (2) that the equation of balance of moments (1) has a first integral that, upon a suitable choice of the origin $\mathbf{O}$, can be written in the form,

$$A(\mathbf{r}'\times\mathbf{r}'')+C(\Omega-\Omega_o)\mathbf{r}'=\mathbf{F}\times\mathbf{r}+\lambda\mathbf{F}, \tag{3}$$

where λ is a constant of integration with the dimension of length. A useful Cartesian coordinate system is that with origin $\mathbf{O}$ and natural basis $\mathbf{i},\mathbf{j},\mathbf{k}$, such that in the expression, $\mathbf{r}(s)=x(s)\mathbf{i}+y(s)\mathbf{j}+z(s)\mathbf{k}$, the unit vector $\mathbf{k}$ is parallel to the (spatially constant) vector $\mathbf{F}$. The corresponding cylindrical coordinates, ρ,ϕ,z, with

$$x=\rho\cos\phi,\quad y=\rho\sin\phi, \tag{4}$$

form a coordinate system introduced by Landau and Lifshitz[16] and employed in (I). In this coordinate system the constraint of inextensibility becomes

$$(\rho')^2=1-u(\phi')^2-(z')^2, \tag{5}$$

where $u=\rho^2$.

From this point on, unless stated otherwise, we shall use $\sqrt{2A/F}$, with $F=|\mathbf{F}|$, as the unit of length, but we shall keep the unit of force the same. (This change affects the values of L, s, $\mathbf{r}$, $\mathbf{M}$, Ω, Ω_o, λ, x, y, z, ρ, and u, but not of $\mathbf{F}$, A, and C.) In the new system of units, Eq. (3) simplifies to

$$\mathbf{t}\times\mathbf{t}'+T\mathbf{t}=2[(\mathbf{k}\times\mathbf{r})+\lambda\mathbf{k}], \tag{6}$$

where

$$T=(C/A)(\Omega-\Omega_o), \tag{7}$$

is a dimensionless number, called the *effective twist density*, that is here independent of s. In (I) it is shown that Eq. (6) implies the relations,

$$z'=a-u, \tag{8}$$

$$\phi'=u^{-1}\left[\frac{T}{2}-\lambda(a-u)\right], \tag{9}$$

$$u'=\pm 2\sqrt{P_3(u)}, \tag{10}$$

in which a is another constant of integration and

$$P_3(u)=-\left[u^3+(\lambda^2-2a)u^2+(a^2-2a\lambda^2+T\lambda-1)u+\left(\frac{T}{2}-a\lambda\right)^2\right]. \tag{11}$$

We write

$$P_3(u)=(u-u_1)(u-u_2)(u_3-u), \tag{12}$$

and number the roots u_i of the cubic polynomial $P_3(u)$ so that $u_1\leqslant u_2\leqslant u_3$. These roots are determined by the triplet (λ,a,T). As the constant term $-[(T/2)-a\lambda]^2$ in $P_3(u)$ is not positive and equals $u_1u_2u_3$, we have $u_1\leqslant 0$. For large u, $P_3(u)$ is negative. As $u=\rho^2$ and Eq. (10) requires that $P_3(u)$ be not negative on solutions of Eq. (1), for each solution the constants λ,a,T must be such that $0\leqslant u_2\leqslant u_3$, and the range of u is contained in the interval $u_2\leqslant u\leqslant u_3$.

Equation (6) yields the following relation[1] between the radial coordinate $\rho(s)$ and the curvature $\kappa(s)$ of $\mathscr{C}$:

$$\kappa^2+T^2=4(\rho^2+\lambda^2). \tag{13}$$

III. ELASTIC ENERGY

In our discussion of the dependence of the elastic energy of a rod on its state, for quantities that have the dimension of length or reciprocal length we shall continue to write s,L,z,κ,Ω, etc., when the unit of length is $\sqrt{2A/F}$, but we shall employ superposed bars, as in $\bar{s}$, $\bar{L}$, etc., when these quantities are measured in conventional (e.g., SI) units. Whereas $\bar{L}$ is the true length of the rod, $L=\bar{L}\sqrt{F/2A}$ depends on the state of the rod, and is defined only for states in which F is independent of s, as is the case at equilibrium.

Let Ψ be the total elastic energy in conventional units of a rod of length $\bar{L}$. In the present theory, whether or not the rod is at equilibrium,

$$\Psi=\Psi_B+\Psi_T, \tag{14}$$

where Ψ_B is the total bending energy,

$$\Psi_B=\frac{1}{2}A\int_{-\bar{L}/2}^{\bar{L}/2}\bar{\kappa}^2 d\bar{s}, \tag{15}$$

and Ψ_T the total twist energy,

$$\Psi_T=\frac{1}{2}C\int_{-\bar{L}/2}^{\bar{L}/2}(\bar{\Omega}-\bar{\Omega}_0)^2 d\bar{s}. \tag{16}$$

We define Φ_B, Φ_T, and Φ by

$$\Phi_B=\bar{L}\Psi_B/A,\quad \Phi_T=\bar{L}\Psi_T/A,\quad \Phi=\Phi_B+\Phi_T=\bar{L}\Psi/A. \tag{17}$$

We now consider equilibrium states, and we write ζ for the unit-free quantity defined as the ratio of the difference in z-coordinates of the end points of the rod to the length of the rod,

$$\zeta=[z(L/2)-z(-L/2)]/L. \tag{18}$$

By using Eqs. (8) and (13), one can derive, after some algebra, the following expressions for the elastic energy at equilibrium:

$$\Phi=2L^2\left[a+\lambda^2-\zeta+\frac{1}{4}\left(\frac{A}{C}-1\right)T^2\right], \tag{19}$$

$$\Phi_B=2L^2\left(a+\lambda^2-\zeta-\frac{1}{4}T^2\right), \tag{20}$$

$$\Phi_T=\frac{1}{2}(A/C)(LT)^2. \tag{21}$$

Of course, although the values of Φ_B, Φ_T, and Φ depend on the state of the rod, the units in which they are measured do not.

For rods subject to geometric end conditions, the boundary data consist of η, the ratio of the distance in space between the end points of $\mathscr{C}$ to the length of $\mathscr{C}$,

$$\eta=|\mathbf{r}(-L/2)-\mathbf{r}(L/2)|/L, \tag{22}$$

and three angular coordinates that specify the orientation of the tangent vectors $\mathbf{t}$ at the end points of $\mathscr{C}$. To describe the latter, one can introduce a unit vector $\boldsymbol{\nu}$ defined so that it points from the end point of $\mathscr{C}$ where $s=L/2$ to that where $s=-L/2$,

$$\boldsymbol{\nu}=\frac{\mathbf{r}(-L/2)-\mathbf{r}(L/2)}{|\mathbf{r}(-L/2)-\mathbf{r}(L/2)|}. \tag{23}$$

(We note that $\boldsymbol{\nu}$ enters the equation

$$\zeta=-\eta\boldsymbol{\nu}\cdot\mathbf{k} \tag{24}$$

relating η to the quantity ζ in the expressions for Φ and Φ_B.) The angles, α_+, α_-, between $\boldsymbol{\nu}$ and the tangents $\mathbf{t}(L/2)$ and $\mathbf{t}(-L/2)$ are given by

$$\cos\alpha_\pm=\boldsymbol{\nu}\cdot\mathbf{t}(\pm L/2), \tag{25}$$

and the dihedral angle μ between the plane containing vectors $\mathbf{t}(-L/2)$ and $\boldsymbol{\nu}$ and the plane containing $\mathbf{t}(L/2)$ and $\boldsymbol{\nu}$ is defined by the relations

$$\sin\mu=\frac{[\mathbf{t}(L/2)\times\mathbf{t}(-L/2)]\cdot\boldsymbol{\nu}}{|\boldsymbol{\nu}\times\mathbf{t}(L/2)||\boldsymbol{\nu}\times\mathbf{t}(-L/2)|},\qquad \cos\mu=\frac{[\mathbf{t}(L/2)\times\boldsymbol{\nu}]\cdot[\boldsymbol{\nu}\times\mathbf{t}(-L/2)]}{|\boldsymbol{\nu}\times\mathbf{t}(L/2)||\boldsymbol{\nu}\times\mathbf{t}(-L/2)|}. \tag{26}$$

IV. EXACT SOLUTIONS FOR SYMMETRIC END CONDITIONS

We here treat cases in which the end conditions are symmetric in the sense that the angle between $\boldsymbol{\nu}$ and $\mathbf{t}$ is the same at each end of the rod,

$$\alpha_+=\alpha_-=\alpha. \tag{27}$$

When this symmetry holds, the curvature of $\mathscr{C}$ and the coordinate $\rho(s)$ have extrema at the midpoint of $\mathscr{C}$, i.e., at $s=0$. In each of the examples given in this paper these extrema are maximum values. Let $\mathscr{\ell}$ be the straight line determined by the midpoint of $\mathscr{C}$ and the midpoint of the straight line segment connecting the ends of $\mathscr{C}$. Equation (27) implies that $\mathscr{\ell}$ intersects the z-axis and is perpendicular to both $\boldsymbol{\nu}$ and $\mathbf{k}$. The origin $\mathbf{O}$ can be chosen so that it coincides with the intersection of $\mathscr{\ell}$ and the z-axis, and once such a choice is made, one can choose the x-axis so that it coincides with $\mathscr{\ell}$.

TABLE I. Properties of axial curves for nicked DNA.

	α	$\lambda\times10^{-3}$	a	$L/2$	Φ	$\cos\gamma$
			Figure 1: $\eta=0.025$, $\beta=2°$			
S_I	80.0°	−3.621	0.442 15	2.043 8	15.604	−0.990 83
S_{II}	94.5°	−22.602	0.459 06	2.201 4	17.933	−0.100 95
S_{III}	94.7°	−22.758	0.462 01	2.200 3	17.937	−0.005 49
S_{IV}	94.9°	−22.710	0.464 97	2.198 9	17.937	0.089 99
S_V	109.4°	−3.940	0.516 23	2.016 7	15.992	0.990 25
U_I	80.0°	2.560	0.498 82	2.401 6	21.875	0.990 65
U_{II}	94.5°	21.543	0.464 79	2.250 6	18.782	0.087 71
U_{III}	94.7°	21.589	0.461 73	2.251 8	18.783	−0.016 18
U_{IV}	94.9°	21.395	0.458 71	2.253 2	18.788	−0.119 62
U_V	109.4°	2.480	0.448 75	2.423 5	22.249	−0.990 87
			Figure 4: $\eta=0.025$, $\beta=0°$			
	α	λ	a	$L/2$	Φ	$\cos\gamma$
A_u	94.692°	0	0.432 66	2.239 2	18.358	−1
A_c	94.692°	0	0.492 88	2.214 6	18.358	1
			Figure 4: $\eta=0.383\,38$, $\beta=0°$			
	α	λ	a	$L/2$	Φ	$\cos\gamma$
B_u	170.970°	0	0.091 82	2.604 5	25.787	−1
B_c	170.970°	0	1.000 00	2.286 4	25.787	1

We choose **O** and the x-axis in this manner and note that then $\mathbf{t}(L/2)\cdot(\boldsymbol{\nu}\times\mathbf{i})=\mathbf{t}(-L/2)\cdot(\boldsymbol{\nu}\times\mathbf{i})$. The angle β, defined by

$$\beta=\arcsin[\mathbf{t}(L/2)\cdot(\boldsymbol{\nu}\times\mathbf{i})]=\arcsin[\mathbf{t}(-L/2)\cdot(\boldsymbol{\nu}\times\mathbf{i})], \tag{28}$$

and introduced in (I), will be employed here in place of μ, for when Eq. (27) holds β measures the inclination of $\mathbf{t}(L/2)$ and $\mathbf{t}(-L/2)$ from the plane $\mathscr{P}$ in space that contains the points with radial vectors $\mathbf{r}(-L/2)$, $\mathbf{r}(L/2)$, and $\mathbf{r}(0)$. Thus boundary data for the problems we treat are described by a triplet (η,α,β). [If Eq. (27) were not assumed, a natural description of the boundary data would be given by the list $(\eta,\alpha_+,\alpha_-,\mu)$.]

The symmetry condition (27) and our choice of **O** and the x-axis imply that for sufficiently small values of β and for values of α near enough to 90°, β/μ is approximately $-1/2$. They also imply that, as functions of s, x is an even function, and y and z are odd functions.

When Eq. (27) holds, Eqs. (8)–(12) yield the following expressions[1] for $\mathscr{C}$ in the coordinate system ρ,ϕ,z:

$$\rho^2=u=u_3-(u_3-u_2)\mathrm{sn}^2(s\sqrt{u_3-u_1}), \tag{29}$$

$$\phi=\lambda s+\frac{[(T/2)-\lambda a]\Pi(n;\psi|m)}{u_3\sqrt{u_3-u_1}}, \tag{30}$$

$$z=(a-u_1)s-\sqrt{u_3-u_1}\ \mathrm{E}(\psi|m); \tag{31}$$

here

$$m=(u_3-u_2)/(u_3-u_1),\quad n=(u_3-u_2)/u_3, \tag{32}$$

sn is a Jacobi elliptic function with parameter m given by (32),

$$\psi=\arcsin(\mathrm{sn}(s\sqrt{u_3-u_1})), \tag{33}$$

and Π and E are elliptic integrals (we use a notation close to that of Ref. 17),

$$\Pi(n;\psi|m)=\int_0^\psi\frac{d\omega}{(1-n\ \sin^2\omega)\sqrt{1-m\ \sin^2\omega}}, \tag{34}$$

$$\mathrm{E}(\psi|m)=\int_0^\psi(1-m\ \sin^2\omega)^{1/2}d\omega. \tag{35}$$

Equation (33) can be written,

$$s=\mp\frac{\mathrm{F}(\psi|m)}{\sqrt{u_3-u_1}},\quad \mathrm{F}(\psi|m)=\int_0^\psi\frac{d\omega}{\sqrt{1-m\ \sin^2\omega}}. \tag{36}$$

Equations (29),(30),(31) for the cylindrical coordinates $\rho(s),\phi(s),z(s)$ yield, by Eqs. (4), explicit formulas for the Cartesian coordinates $x(s),y(s),z(s)$.

The relations (13) and (29) yield an explicit formula for $\kappa^2(s)$,

$$\kappa^2=4[\lambda^2+u_3-(u_3-u_2)\mathrm{sn}^2(s\sqrt{u_3-u_1})]-T^2. \tag{37}$$

[See Eq. (4.10) of Ref. 5 for the generalization of this expression to traveling waves; for such waves, as for equilibrium states, κ^2 and ρ^2 are affine functions of $\mathrm{sn}^2(s\sqrt{u_3-u_1})$.]

V. NICKED DNA

Consider now a finite segment of duplex DNA which has had one of its two strands nicked in at least one place, which in the present theory means that the constitutive relation (2) is replaced by the two equations

$$\Omega=\Omega_o,\quad \mathbf{M}=A(\mathbf{t}\times\mathbf{t}'), \tag{38}$$

and hence that the effective twist density T in Eqs. (9), (11), and (13) is zero. The end conditions are assumed such that the symmetry condition (27) holds and that the numbers η, α, and β are specified. Here, as in Sec. IV, we choose the x-axis to be perpendicular to $\boldsymbol{\nu}$, and, like $\boldsymbol{\nu}$, to lie in the plane

$\mathscr{P}$ determined by the points of $\mathscr{C}$ at $s=0$, $-L/2$, and $+L/2$. We recall that η is a dimensionless measure of the separation of the end points of $\mathscr{C}$ and that α is the angle that the tangent at each end point of $\mathscr{C}$ makes with $\boldsymbol{\nu}$; β is the (signed) angle of inclination of both such tangents from the plane $\mathscr{P}$. Here we take β to be nonzero. (When $T=0$, if β is set equal to zero, all of $\mathscr{C}$ will lie in the plane $\mathscr{P}$. This case is discussed in Sec. VI, where we present a way of obtaining planar configurations as limiting cases of configurations of nicked DNA with $\beta\neq 0$.)

To verify that a pair of integration constants (λ,a) is compatible with a triplet (η,α,β), i.e., yields an axial curve $\mathscr{C}$ with

$$|\mathbf{r}(-L/2)-\mathbf{r}(L/2)|/L=\eta, \tag{39}$$

$$\boldsymbol{\nu}\cdot\mathbf{t}(L/2)=\boldsymbol{\nu}\cdot\mathbf{t}(-L/2)=\cos\,\alpha, \tag{40}$$

$$\mathbf{t}(L/2)\cdot(\boldsymbol{\nu}\times\mathbf{i})=\mathbf{t}(-L/2)\cdot(\boldsymbol{\nu}\times\mathbf{i})=\sin\,\beta, \tag{41}$$

one must know also $L=\bar{L}\sqrt{F/2A}$. Thus for $T=0$ the problem of finding an equilibrium configuration consistent with given end conditions is one of finding a triplet (λ,a,L) for which Eqs. (39)–(41) hold for the specified (η,α,β). To evaluate the left-hand sides of Eqs. (39)–(41) for a triplet (λ,a,L), it suffices to know the Cartesian components of $\mathbf{r}$ and $\mathbf{t}=\mathbf{r}'$ at $s=\pm L/2$; to calculate these components, we compute the roots u_i of P_3 in Eqs. (11) and (12) with $T=0$ and obtain x, y, and z at $s=\pm L/2$ from Eqs. (4) and (29)–(31); z' is obtained from Eq. (8); x' and y' are obtained from the relations

$$x'=\frac{u'}{2u}\,x-\phi' y,\quad y'=\frac{u'}{2u}\,y+\phi' x, \tag{42}$$

in which ϕ' is as in Eq. (9) and, by Eq. (29),

$$u'=-2(u_3-u_2)\sqrt{u_3-u_1}\;\mathrm{sn}t\;\mathrm{cn}t\;\mathrm{dn}t, \tag{43}$$

with $t=s\sqrt{u_3-u_1}$.

Thus, the mapping $(\lambda,a,L)\mapsto(\eta,\alpha,\beta)$ can be evaluated with ease. One can automate the procedure of inverting this mapping so as to obtain (λ,a,L) and hence $\mathscr{C}$ [via Eqs. (4), (29)–(31)] from the boundary data (η,α,β). There are ranges of the triplet (η,α,β) for which the inverse (λ,a,L) is not unique. For small values of β, there are at least two inverses (λ,a,L) for each triplet (η,α,β). In Table I we list, for $\eta=0.025$, $\beta=2°$, and five values of α, two inverse triplets (λ,a,L) and the corresponding values of Φ obtained from Eq. (19), which equation here reduces to

$$\Phi=\Phi_B=2L^2(a+\lambda^2-\zeta). \tag{44}$$

Calculated axial curves $\mathscr{C}$ corresponding to the data of Table I for $\eta=0.025$ and $\beta=2°$ are shown in Fig. 1. The curves with the smaller values of Φ, and hence of Ψ, are labeled $S_I,...,S_V$; those with the higher values are labeled $U_I,...,U_V$. (When presenting calculated curves $\mathscr{C}$ corresponding to equilibrium configurations with equal values of η but other differences, as in the case of Fig. 1, we normalize the scale of distance so that the curves have equal values of true length, $\bar{L}$.)

Figure 2(A) contains graphs of Φ as a function of α for $\eta=0.025$ with the magnitude of the angle β set equal to 2° and to 0°; ($\beta=0°$ corresponds to planar configurations discussed below). Advantages of working with Φ are (i) Φ is determined, in the present case, by (λ,a,L), and (ii) although $\bar{L}$ cannot be calculated when only η, α, and β are given, one can assert that for a single segment, or for two segments with equal values of A and L, the larger value of Φ corresponds to the larger value of Ψ.

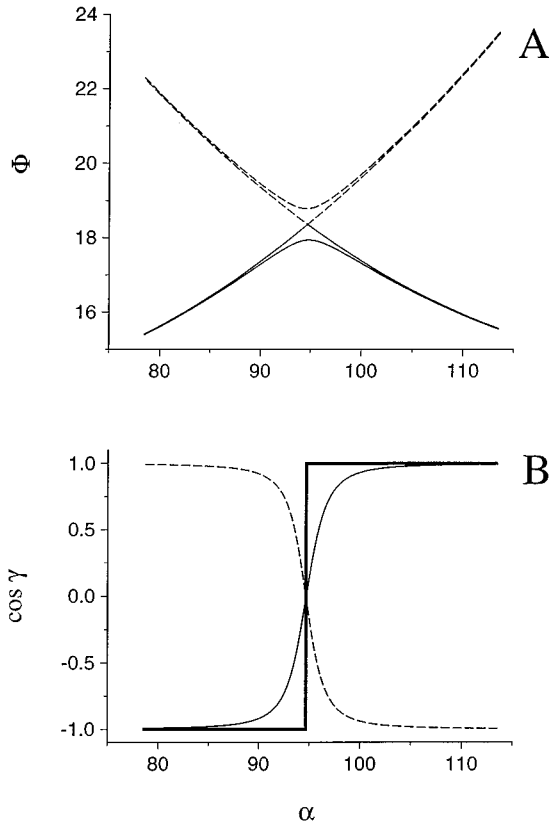

FIG. 2. (A) Elastic energy Φ vs α (in degrees) for $\eta=0.025$; —, stable configurations; – – –, unstable configurations. The smooth curves correspond to $|\beta|=2°$; the curves with sharp bends at $\alpha=94.692°$ correspond to $\beta=0°$, i.e., to planar loops. When $\eta=0.025$, planar crossed loops are stable for $\alpha>94.692°$ and planar uncrossed loops are stable for $\alpha<94.692°$. (B) Calculated values of $\cos\gamma$ as a function of α for $\eta=0.025$; —, stable configurations with $|\beta|=2°$; – – –, unstable configurations with $|\beta|=2°$. The heavy solid step function is the limit for stable configurations as $|\beta|\to 0°$, i.e., corresponds to stable planar loops.

For a nicked DNA segment subject to strong anchoring end conditions of the type considered here, of the two equilibrium configurations we discuss, the one with the lower value of Ψ is mechanically stable in the sense that it gives a local minimum to the bending energy (for the class of nonequilibrium perturbations obeying the same end conditions); the configuration with the higher value is unstable in the sense that there are small perturbations of it (of the same type) that result in a decrease in bending energy. The proof of this result, as it requires the assembly of a different mathematical apparatus from that employed for the calculations presented here, will be given in a subsequent paper. The result is mentioned here to explain why, in the present case of a nicked segment with more than one equilibrium configuration obeying specified strong anchoring end conditions, we take the configuration of lowest elastic energy to be physi-

cally relevant, call that configuration *stable* and those of higher energy *unstable*, and use labels (S and U) that are derived from this appellation.

For the boundary data (η,α,β) for which values of (λ,a,L) are given in Table I, the mapping $(\lambda,a,L)\mapsto(\eta,\alpha,\beta)$ has more than two inverses, but the other triplets (λ,a,L) correspond to unstable configurations with larger values of the energy Φ than those of the configurations we discuss.

Let γ be the angle that the tangent at the midpoint of $\mathscr{C}$ makes with the line connecting the end points of $\mathscr{C}$ so that, by Eq. (23),

$$\mathbf{t}(0)\cdot\boldsymbol{\nu}=\cos\,\gamma. \tag{45}$$

Values of γ for the configurations drawn in Fig. 1 are given in Table I, and Fig. 2(B) contains graphs of $\cos\gamma$ vs α corresponding to the energy curves in Fig. 2(A).

In a complete sequence of configurations of the type seen in Fig. 1, where η and β are fixed at small values, as α decreases through an appropriate range of values, $\mathbf{t}(0)$ rotates through approximately 180° with $\mathbf{i}$ its axis of rotation. When α passes a value that is near to 90° (for η and β sufficiently small), the rotation of $\mathbf{t}(0)$ with changes in α is rapid. We call such changes in configuration "180° loop flips." (The interested reader will find it not difficult to show that a length of music wire grasped at its ends can be made to undergo such "loop flips." In such experiments with music wire it is found that the configurations labeled S in Fig. 1 are indeed stable, but those labeled U are not, provided the inability of nicked DNA to support a twisting moment is mimicked by permitting free rotation about the tangent at one or both of the two points at which the rod is grasped.)

VI. PLANAR CONFIGURATIONS AS LIMITING CASES

We turn now to cases in which end points of $\mathscr{C}$ and the tangent vectors, $\mathbf{t}(-L/2)$, $\mathbf{t}(L/2)$, all lie in the plane $\mathscr{P}$. Whether or not the DNA segment is in a nicked state, if it is in equilibrium with zero effective twist density, it can have torsion-free (i.e., planar) configurations compatible with the prescribed values of $\mathbf{r}(-L/2)$, $\mathbf{r}(L/2)$, $\mathbf{t}(-L/2)$, and $\mathbf{t}(L/2)$, and these can be found by standard methods of the theory of the elastica (vid., e.g., the treatise of Love[18]) or by examination of the restriction to finite intervals of results in the theory of traveling waves of pure flexure.[19] Moreover, it follows from a familiar theorem in Kirchhoff's theory that for an (unnicked) homogeneous, naturally straight rod, each planar equilibrium configuration that is not trivial (i.e., that does not have constant curvature and hence is neither circular nor straight) must give rise to a zero twisting moment everywhere, and therefore must be such that the Eqs. (38) hold in that configuration. Thus, each nontrivial planar configuration of a DNA segment obeying our theory, whether nicked or not, can be treated as a small $|\beta|$ limit of results given above for a nicked segment.

It is not difficult to show that in the limit as $\beta\to0$ with η and α fixed, for a nicked segment the constant force vector $\mathbf{F}$ lies in the plane $\mathscr{P}$, and hence λ, as well as T, is zero. Thus, $P_3(u)$ in Eq. (11) has at most two nonzero roots, and these have the values $a+1$ and $a-1$. In the terminology of the classical theory of the elastica, the only possibilities are the following: if the curve $\mathscr{C}$ is *inflexional*, i.e., is a segment of an elastic curve that has an inflexion point, then

$$a<1,\;\; u_1=a-1,\;\; u_2=0,\;\; u_3=a+1; \tag{46}$$

if $\mathscr{C}$ is *noninflexional*, then

$$a>1,\;\; u_1=0,\;\; u_2=a-1,\;\; u_3=a+1; \tag{47}$$

if $\mathscr{C}$ is intermediate between inflexional and noninflexional, and hence is a segment of an "Euler loop," i.e., an infinite elastic curve with inflexion points at infinity and only at infinity, then

$$a=1,\;\; u_1=u_2=0,\;\; u_3=2. \tag{48}$$

For $T=0$, in a limit in which λ becomes zero, φ equals 0 or π, and, in view of Eqs. (29)–(37), (4), and the identity $\mathrm{sn}^2+\mathrm{cn}^2=1$,

$$\frac{1}{4}\,\kappa^2=u=u_3-(u_3-u_2)\mathrm{sn}^2(s\sqrt{u_3-u_1}), \tag{49}$$

$$x=\pm[u_2+(u_3-u_2)\mathrm{cn}^2(s\sqrt{u_3-u_1})]^{1/2}=\pm\rho, \tag{50}$$

$$y=0, \tag{51}$$

$$\begin{aligned} &z=(a-u_1)s-\sqrt{u_3-u_1}\;\mathrm{E}(\psi|m),\\ &\psi=\arcsin(\mathrm{sn}(s,\sqrt{u_3-u_1})). \end{aligned} \tag{52}$$

Here again the modulus m is given by (32). In Eq. (50) the sign of x is chosen to agree with the sign of $\mathrm{cn}(s\sqrt{u_3-u_1})$.

When $\mathscr{C}$ is inflexional, $u_2=0$ and Eq. (50) reduces to

$$x=(a+1)^{1/2}\;\mathrm{cn}(s\sqrt{2}). \tag{53}$$

When $\mathscr{C}$ is noninflexional, $u_1=0$ and

$$x=\pm[2\;\mathrm{cn}^2(s\sqrt{a+1})+a-1]^{1/2}. \tag{54}$$

In the special case in which $\mathscr{C}$ is a segment of an Euler loop, Eqs. (50) and (52) reduce to

$$x=\pm\sqrt{2}\;\mathrm{sech}(s\sqrt{2}) \tag{55}$$

and

$$z=s-\sqrt{2}\;\tanh(s\sqrt{2}). \tag{56}$$

When $\beta=0°$ with $T=0$, $\cos\gamma$ can be only $+1$ or -1. Thus the graphs seen in Fig. 2(B) become step functions in the limit where $\beta=0°$. When $|\beta|=2°$, for $\cos\gamma$ near to $+1$ or -1, as is the case for the configurations $\mathrm{S_I}$, $\mathrm{S_V}$ of Fig. 1, projections on the plane $\mathscr{P}$ are almost indistinguishable from those that correspond to the same values of η and α and have $\beta=0°$. In such cases of small $|\beta|$, we refer to configurations of the type $\mathrm{S_V}$, $\mathrm{U_I}$ as *crossed* (or, more precisely, *singly crossed*) and to those of type $\mathrm{S_I}$, $\mathrm{U_V}$ as *uncrossed*. Configurations such as $\mathrm{S_{II}}$,$\mathrm{S_{III}}$,$\mathrm{S_{IV}}$ and $\mathrm{U_{II}}$,$\mathrm{U_{III}}$,$\mathrm{U_{IV}}$ of Fig. 1, i.e., configurations that are intermediate between crossed and uncrossed configurations, are not planar and do not occur with $\beta=0°$.

Since

$$u(0)=u_3, \tag{57}$$

and, by Eq. (8), $\mathbf{t}(0)\cdot\mathbf{k}=z'(0)=a-u_3$, when $\beta=0°$ with $T=0$, it follows from Eqs. (46)–(48) that

$$\mathbf{t}(0)\cdot\mathbf{k}=-1. \tag{58}$$

In this limit of small $|\beta|$, Eq. (24) becomes $\zeta=\eta\boldsymbol{\nu}\cdot\mathbf{t}(0)$, and as the tangent at the midpoint of $\mathscr{C}$ is parallel or antiparallel to $\boldsymbol{\nu}$ in accord with whether the configuration is uncrossed or crossed, the expression (44) for the elastic energy in units of A/L here reduces to the remarkably simple assertion that

$$\Phi=2L^2(a+\eta) \quad \text{for uncrossed } \mathscr{C}, \tag{59a}$$

$$\Phi=2L^2(a-\eta) \quad \text{for singly crossed } \mathscr{C}. \tag{59b}$$

The graphs of Φ vs α for $\beta=0°$ seen in Fig. 2(A) were computed using these relations. Examples of multiply crossed planar configurations with $T=0$ and specified values of η and α can be constructed using known examples of periodic elastic curves (such as those shown in Figs. 2 and 3 of Ref. 19), but these have far larger values of Φ and hence Ψ than the corresponding uncrossed and singly crossed configurations considered here.

In the limit of small $|\beta|$, a (singly) crossed DNA segment touches itself at points with arc-length coordinates s_+, s_- that are roots of the equations,

$$z(s_+)=z(s_-),\ \ x(s_+)=x(s_-). \tag{60}$$

As symmetry of $\mathscr{C}$ about the x-axis implies that $s_-=-s_+$ and that z is an odd function of s, the number s_+ can be found by looking for the unique solution of the equation

$$z(s_+)=0 \tag{61}$$

with $0<s_+<L/2$. In view of Eqs. (52), this last equation can be written

$$\begin{aligned}&(a-u_1)s_+=\sqrt{u_3-u_1}\ \mathrm{E}(\psi_+|m),\\ &\psi_+=\arcsin(\mathrm{sn}(s_+\sqrt{u_3-u_1})),\end{aligned} \tag{62}$$

and hence when the pair (η,α) is given one can calculate, for the corresponding planar crossed configuration, the dimensionless number,

$$\Gamma=2s_+/L, \tag{63}$$

that equals the fraction of the total length $\bar{L}$ of the DNA segment that is contained in the new closed loop formed by the crossover, i.e., the fraction with s in the interval $s_-\leqslant s\leqslant s_+$, or with $\bar{s}_-\leqslant\bar{s}\leqslant\bar{s}_+$

Let us write θ for the angle that $\mathbf{t}$ makes with $\mathbf{k}$. In a planar crossed configuration obeying our symmetric boundary conditions, the angle between the vectors $\mathbf{t}(s_+)$ and $\mathbf{t}(s_-)$, called the *crossing angle*, is

$$\chi=\theta(s_+)-\theta(s_-)=2\,\theta(s_+). \tag{64}$$

As $\cos\theta=z'$, Eqs. (8), (29), and (33) yield

$$\begin{aligned}\cos(\chi/2)&=a-u_3+(u_3-u_2)\mathrm{sn}^2(s_+\sqrt{u_3-u_1})\\ &=a-u_3+(u_3-u_2)\sin^2\ \psi_+.\end{aligned} \tag{65}$$

In the case in which $\mathscr{C}$ is inflexional, i.e., in which (46) holds, by use of Eq. (36) and the identity, $\mathrm{dn}^2+m\ \mathrm{sn}^2=1$ with $m=(a+1)/2$, Eq. (65) can be written

$$\cos(\chi/2)=1-2\ \mathrm{dn}^2(s_+\sqrt{2}). \tag{66}$$

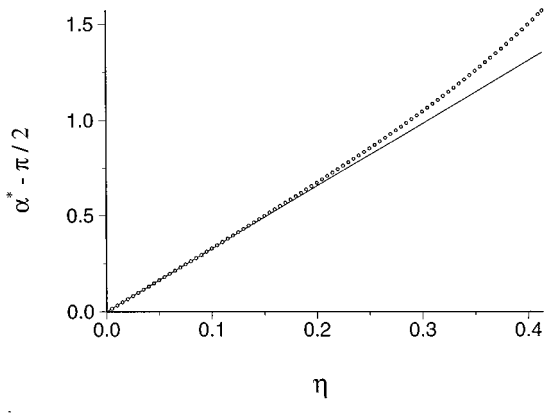

FIG. 3. The critical value α^* of α (in radians) at which crossed and uncrossed planar loops have equal energy as a function of η. The circles show results obtained by numerical solution of the equation $\Phi_u=\Phi_c$. The straight line is the linear approximation $\alpha^*=\pi/2+3.274\eta$.

In the case in which Eq. (47) holds and $\mathscr{C}$ is noninflexional, we have

$$\cos(\chi/2)=2\ \mathrm{sn}^2(s_+\sqrt{2/m})-1, \tag{67}$$

and $m=2/(a+1)$. In the special case of the Euler loop, i.e., of Eq. (48),

$$\cos(\chi/2)=1-2\ \mathrm{sech}^2(s_+\sqrt{2}). \tag{68}$$

In the planar case, the mapping $(\lambda,a,L)\mapsto(\eta,\alpha,\beta)$ reduces to $(a,L)\mapsto(\eta,\alpha)$ and can be evaluated by using Eqs. (8), (42), (43), (49), (50), and (52) to calculate the left-hand sides of Eqs. (39) and (40). Once this is done, the mapping $(a,L)\mapsto(\eta,\alpha)$ can be inverted to obtain, for specified boundary data (η,α), two pairs of parameters, (a_u,L_u) and (a_c,L_c), that correspond to uncrossed and (singly) crossed configurations of $\mathscr{C}$. These two configurations for the data (η,α) have elastic energies $\Phi_u=2L_u^2(a_u+\eta)$ and $\Phi_c=2L_c^2(a_c-\eta)$, respectively. We have found that for each value of η in an interval of the form $0<\eta<\eta_M$, there is a critical value, $\alpha^*(\eta)$, of α such that $\Phi_u=\Phi_c$ for the pair $(\eta,\ \alpha^*(\eta))$; α^* decreases to 90° in the limit of small η. Our calculations give

$$\eta_M=0.4136. \tag{69}$$

In view of remarks made in Sec. V about the stability of configurations with the same end conditions (η,α,β) but different values of Ψ, we can assert that a planar equilibrium configuration of a nicked segment with $0<\eta<\eta_M$ is stable if it is uncrossed with α less than α^* or if it is crossed with α greater than α^*.

We have evaluated the dependence of α^* on η by numerically solving the equation $\Phi_u=\Phi_c$ for α at specified values of η with $0<\eta<\eta_M$. The results are shown as open circles in Fig. 3. As that figure makes clear, for $0\leqslant\eta<0.1$, $\alpha^*(\eta)$ in radians is given to a good approximation by the linear relation

$$\alpha^*=\pi/2+3.274\,\eta. \tag{70}$$

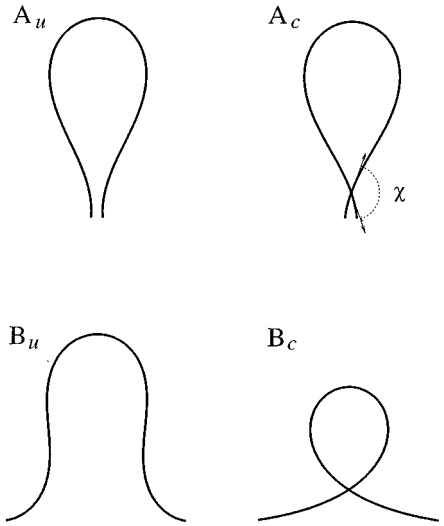

FIG. 4. Equal energy planar loops for two pairs $(\eta, \alpha^*(\eta))$. The values of η, $\alpha^*(\eta)$, and other parameters are given in Table I. B_c is a segment of a Euler loop and hence is given by the Eqs. (55) and (56).

Thus, we can assert that *for η less than 0.1, a stable planar equilibrium configuration is crossed or uncrossed in accord with whether the angle α exceeds or is less than $\pi/2 + 3.274\eta$.*

Two pairs of crossed and uncrossed equal energy configurations are shown in Fig. 4; for A_u and A_c, $\eta=0.025$; for B_u and B_c, η was chosen to be η_E, with

$$\eta_E = 0.383\ 38, \tag{71}$$

the value of η such that the crossed loop with $\alpha=\alpha^*(\eta_E)$ has $a=1$ and hence is a segment of a Euler loop.

Figure 5 contains graphs of the ratio Γ, defined in Eq. (63), and the crossing angle χ, defined in Eq. (64), as functions of η. The calculations are based on Eqs. (62) and (65) for crossed planar loops. For this figure the range of η is $0<\eta<\eta_M$. The dashed lines labeled a, b, and c correspond to fixed values of α. Along the heavy solid line α is equal to $\alpha^*(\eta)$. When α is chosen to be $\alpha^*(\eta)$, the derivatives of Γ and χ with respect to η are discontinuous at $\eta=\eta_E$, and, whereas the uncrossed loop of an equal energy pair is inflexional for each η in $0<\eta<\eta_M$, the corresponding crossed loop is inflexional for $\eta<\eta_E$ and noninflexional for $\eta>\eta_E$.

The curves shown in Fig. 6 are graphs of Φ vs $\cos\alpha$ for stable planar configurations and were calculated using Eqs. (59a) and (59b). The light solid curves labeled a, b, and c at their apexes correspond, respectively, to $\eta=0.1$, $\eta=0.05$, and the limit as $\eta\to 0$; in each case, on the part of the curve to the left of its apex, $\mathscr{C}$ is crossed, and on the part to the right, $\mathscr{C}$ is uncrossed. The curve c, corresponding to the limit of small η, is symmetric about $\cos\alpha=0$; for in that limit the distinction between crossed and uncrossed configurations disappears. As $\eta\to 0$ with α held fixed, the crossing point of a singly crossed loop approaches the end points $s=\pm L/2$.

The heavy solid curve in Fig. 6 is a graph of Φ vs $\cos\alpha$ for values of η such that $\alpha=\alpha^*(\eta)$, i.e., such that Φ does not depend on whether the configuration is crossed.

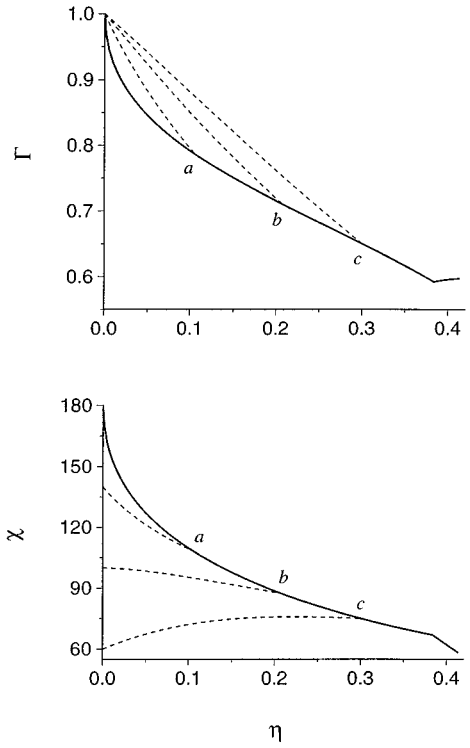

FIG. 5. Upper graph: The fraction Γ of the total length of a nicked planar DNA segment contained in a stable closed loop formed by a crossover as a function of η. Lower graph: The crossing angle χ as a function of η. In both graphs, on the heavy solid curve $\alpha=\alpha^*(\eta)$; α is constant on the dashed curves labeled a,b,c: for a, $\alpha=110°$; for b, $\alpha=130°$; for c, $\alpha=150°$.

It is clear from Fig. 6 that, for each fixed value of η in the interval $0<\eta<\eta_M$, the graph of Φ vs $\cos\alpha$ has two local minima. The minimum on the left corresponds to a configuration that is crossed and the other to one that is not. If we were to replace our strong anchoring end conditions for nicked segments by end conditions that amount to specifying only η and leaving α to be free, the stable configurations

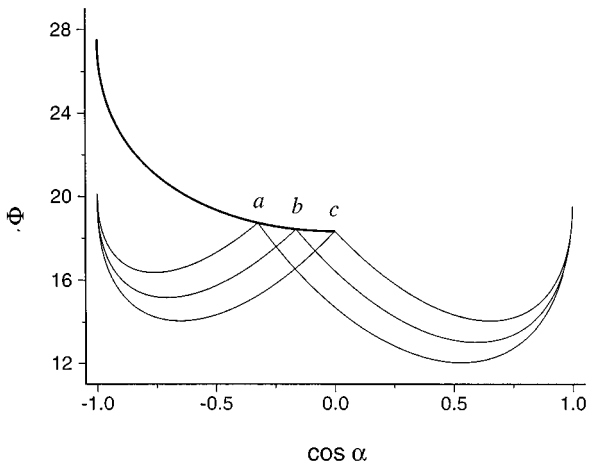

FIG. 6. The elastic energy Φ vs $\cos\alpha$ for stable planar loops. On the light solid curves labeled a,b,c, at their apexes, η is constant; for a, $\eta=0.1$; for b, $\eta=0.05$; c corresponds to the limit in which $\eta=0$. On the heavy solid curve, η is such that $\alpha=\alpha^*(\eta)$.

would correspond to the minima seen in the figure, and for each $\eta < \eta_M$ there would be two stable configurations, one crossed and one uncrossed.

For a singly crossed planar loop with self contact points defined as in Eqs. (60), the crossing angle χ determines, to within a similarity transformation, the shape of the closed part $\mathscr{C}^P$ of $\mathscr{C}$ for which the range of s is $s_- \leqslant s \leqslant s_+$. In particular, neither $\mathscr{C}^P$ nor the elastic energy Φ^P (in units of A/L) of a rod P of length $L = \bar{s}_+ - \bar{s}_-$ that is at equilibrium with $\mathscr{C}^P$ as its axial curve is affected by the presence or absence of stability of the crossed equilibrium configuration of a rod that contains P as a subbody. The curve in Fig. 6 labeled c (at its apex) and described as a limit as $\eta \to 0$, gives Φ^P as a function of $\cos(\chi/2)$, provided we identify χ with 2α in that limit.

ACKNOWLEDGMENTS

We thank Wilma K. Olson for valuable discussions and Andrei Fedorov for help in creating an efficient numerical scheme for inversion of the mapping $(\lambda, a, L) \mapsto (\eta, \alpha, \beta)$. This research was supported by the National Science Foundation under Grant No. DMS-94-04580, by the United States Public Health Service under Grant No. GM34809, and by the Donors of the Petroleum Research Fund, administered by the American Chemical Society.

[1] I. Tobias, B. D. Coleman, and W. K. Olson, J. Chem. Phys. **101**, 10 990 (1994).
[2] G. Kirchhoff, J. F. Reine Angew. Math. (Crelle) **56**, 285 (1859).
[3] G. Kirchhoff, *Vorlesungen über Mathematische Physik, Mechanik, Vorl. 28* (Tuebner, Leipzig, 1876).
[4] E. H. Dill, Arch. Hist. Exact. Sci. **44**, 1 (1992).
[5] B. D. Coleman, E. H. Dill, M. Lembo, Z. Lu, and I. Tobias, Arch. Rational Mech. Anal. **121**, 339 (1993).
[6] L. F. Liu and J. C. Wang, Cell **15**, 979 (1978).
[7] T.-S. Hsieh, in *DNA Topology and Its Biological Effects*, edited by N. R. Cozzarelli and J. C. Wang (Cold Spring Harbor Laboratory, Cold Spring Harbor, NY, 1990), p. 243.
[8] T. J. Richmond, J. T. Finch, B. Rushton, D. Rhodes, and A. Klug, Nature (London) **311**, 532 (1984).
[9] A. Klug, J. T. Finch, and T. J. Richmond, Science **229**, 1109 (1985).
[10] I. Goulet, Y. Zivanovic, and A. Prunell, J. Mol. Biol. **200**, 253 (1988).
[11] Y. Zivanovic, I. Goulet, B. Revet, M. Le Bret, and A. Prunell, J. Mol. Biol. **200**, 267 (1988).
[12] K. E. van Holde, *Chromatin* (Springer, New York, 1989).
[13] S. Adhya, Annu. Rev. Genet. **23**, 227 (1989).
[14] R. Schleif, Annu. Rev. Biochem. **61**, 199 (1992).
[15] K. S. Matthews, Microbiol. Rev. **56**, 123 (1992).
[16] L. D. Landau and E. M. Lifshitz, *Theory of Elasticity*, 3rd ed. (Pergamon, Oxford, 1986).
[17] L. M. Milne-Thomson, in *Handbook of Mathematical Functions*, edited by M. Abramowitz and I. A. Stegun (Dover, New York, 1965), Chaps. 16 and 17, pp. 567 and 589.
[18] A. E. H. Love, *A Treatise on the Mathematical Theory of Elasticity*, 4th ed. (Cambridge University, Cambridge, 1927).
[19] B. D. Coleman and E. H. Dill, J. Acoust. Soc. Am. **91**, 2663 (1992).